Exploring how the fast-slow pace of life continuum and reproductive strategies structure microorganism life history variation

Josje Romeijn[1] & Isabel M. Smallegange[2]

[1] Institute for Biodiversity and Ecosystem Dynamics, University of Amsterdam, PO Box 94240, 1090 GE Amsterdam, The Netherlands

[2] School of Natural & Environmental Sciences, Newcastle University, Newcastle upon Tyne, NE1 7RU, UK

Corresponding author: Isabel M. Smallegange – Isabel.smallegange@newcastle.ac.uk

Abstract

Studying life history strategies in microorganisms can help predict their performance when complex microbial communities can be categorised into groups of organisms with similar strategies. Microorganisms are typically classified as copiotroph or oligotroph, but it has been proven difficult to generalise their life history strategies to broad lineages. Here we tested if the fast-slow continuum and reproductive strategy framework of macro-organismal life histories can be applied to microorganisms. We used demographic and energy budget data from 13 microorganisms (bacteria, fungi, a protist and plant) to examine how generation time, survivorship, growth form, age at maturity, recruitment success, and net reproductive rate structure microbial life histories. We found that 79% of microorganism life-history variation fell along two uncorrelated axes. Like macro-organisms, we found a fast–slow pace of life continuum, including shorter-lived microorganisms at one end, and longer-lived microorganisms that mature later in life at the other. Also, like macro-organisms, we found a second, reproductive strategy axis, with microorganisms with greater lifetime reproductive success and decreased mortality at older age at one end, and microorganisms with the opposite characteristics at the other end. Microorganismal life history strategies did not covary proportionally to their shared evolutionary history. Thus, whereas this work suggests that the macro-organismal fast-slow continuum and reproductive strategy framework could be realistically applied to microorganisms, their life history processes cannot be inferred from patterns in taxonomic composition.

Keywords: demography, fast-slow continuum, dynamic energy budget integral projection model, life history trait, population matrix model, microbes, yeast

Introduction

Different life history strategies capture different combinations of survival, growth and reproduction (demographic) rates of individuals (Stearns 1992) that determine the dynamics of populations. Studying life history strategies in microorganisms can help predict their performance when complex microbial communities can be categorised into groups of organisms with similar strategies. Microorganisms are typically classified along a copiotroph-oligotroph dichotomy (Koch 2001), where copiotrophs grow faster and rely on resource availability, but oligotrophs efficiently exploit resources at the expense of growth rate. In soils, for example, some bacterial phyla are present in greater relative abundance in response to sucrose addition, indicating copiotrophic strategies, whereas other bacterial phyla were either unresponsive or responded negatively, suggesting oligotrophic strategies (Fierer et al. 2007). Ramin and Allison (2019) added a third, maintenance type to the dichotomy. Classifying microorganisms as copiotroph-oligotroph at the phylum level remains prevalent but because bacterial lineages within phyla can have distinct metabolic and ecological roles, more ecologically realistic frameworks are called for (Stone et al. 2023).

In macro-organisms, the majority of life history variation is structured along (i) a fast-slow life history continuum with fast-growing, short-lived species at one end, and slow-growing, long-lived species at the other (Gaillard et al., 1989; Paniw et al., 2018; Capdevila et al., 2020), and (ii) a reproductive strategy axis that for higher plants has iteroparous species that reproduce multiple times as adults at one end and semelparous plants that reproduce only once at the other (Salguero-Gómez et al., 2016; Paniw et al., 2018), whereas for animals this axis is defined by the distribution of age-specific mortality hazards and the spread of reproduction (Healy et al., 2019). We do not know if microorganismal life history variation can be structured along these same life history strategy axes (Evans and Wallenstein 2013) and if this would provide a more ecologically realistic life history framework for microbial ecologists. Such a framework could be useful because processes influenced by microorganisms, e.g., human disease progression (de Vrieze et al., 2013), human-microbe

interactions (Rook et al., 2017) and even ecological strategies of coral species (Meistertzheim et al., 2016), are ultimately governed by the life history dynamics of individual microbial species.

The aim of this explorative study is to investigate main axes of variation in microorganism life histories to offer an alternative life history framework for microbial ecologists to consider when studying the performance of microorganisms. To this end, we first adapted a dynamic energy budget integral projection model (DEB-IPM) (Smallegange et al., 2017) to the microorganism life cycle. Specifically, the microorganismal DEB-IPM is a discrete-time, structured demographic model that takes data on individual cell life histories as input parameters to describe how individual cells grow according to a von Bertalanffy growth curve (Kooijman and Metz, 1984), and reproduce by binary fission to produce two offspring (Margolin 2005) after which individuals die. Individuals are assumed to always suffer a constant background mortality. We parameterised DEB-IPMs for 13 species of microorganism, including bacteria, fungi, a plant and a protist to calculate seven life history traits that inform on schedules of survival, growth, and reproduction (Stearns 1992): generation time, survivorship curve, age at maturity, progressive growth (indicating size increase), retrogressive growth (indicating shrinking), mean recruitment success and net reproductive rate. We then evaluated the variation in these traits along major (life history strategy) axes using a phylogenetically corrected principal component analysis (PCA). By measuring if species life history strategies covary proportionally to their shared evolutionary history, we can assess if the fast-slow reproductive strategy framework can be used to support inferences about life history processes from patterns in taxonomic composition of microorganisms (as has been common practice by microbial ecologists [Stone et al. 2023]).

Methods

Brief description of the DEB-IPM

The demographic function that describes growth in the microorganismal DEB-IPM is derived from the Kooijman-Metz model (Kooiman & Metz 1984). The Kooijman-Metz model assumes that

individual (micro)organisms are isomorphic (body surface area and volume are proportional to squared and cubed length, respectively). The rate at which an individual (cell) ingests food, I, is assumed to be proportional to the maximum ingestion rate I_{max}, the current feeding level Y and body surface area, and hence to the squared length of an organism: $I = I_{max} Y L^2$. Ingested food is assimilated with a constant efficiency ε. A constant fraction κ of assimilated energy is allocated to respiration (the processes by which a cell obtains the oxygen it needs to produce energy and eliminate waste); this respiration energy equals $\kappa \varepsilon I_{max} Y L^2$ and is used to first cover maintenance costs, which are proportional to body volume following ξL^3 (ξ is the proportionality constant relating maintenance energy requirements to cubed length), while the remainder is allocated to somatic growth. This means that, if an individual cell survives from hour t to hour $t + 1$, it grows from length L to length L' following a von Bertalanffy growth curve, $\frac{dL}{dt} = \dot{r}_B (L_m \cdot Y - L)$, where $\dot{r}_B$ is the von Bertalanffy growth rate and $L_m = \kappa \varepsilon I_{max} / \xi$ is the maximum length under conditions of unlimited resource. Both κ and I_{max} are assumed to be constant. However, the role of κ in the DEB-IPM is mostly implicit, as κ is used as input parameter only in the starvation condition (see below), whereas L_m is measured directly from data.

Growth, as described above, as well as survival and reproduction are captured in the DEB-IPM by four fundamental functions to describe the dynamics of a well-mixed population comprising cohorts of individual cells of different sizes (Smallegange et al. 2017): (1) the survival function, $S(L(t))$ (unit: h^{-1}), describing the probability of surviving from hour t to hour t+1; (2) the growth function, $G(L', L(t))$ (unit: h^{-1}), describing the probability that an individual of body length L at hour t grows to length L' at $t + 1$, conditional on survival; (3) the reproduction function, $R\big(L(t)\big)$ (unit: # h^{-1}), giving the number of offspring produced between hour t and $t + 1$ by an individual of length L at hour t; and (4) the parent-offspring function, $D(L', L(t))$ (unit: h^{-1}), the latter which describes the association between the body length of the parent cell L and offspring cell length L' (i.e. to what extent does offspring size depend on parental size). Denoting the number of cells at hour t by

$N(L,t)$ means that the dynamics of the cell length number distribution from hour t to $t + 1$ can be written as:

$$N(L',t+1) = \int_{\Omega} \left[D(L',L(t))R\big(L(t)\big) + G(L',L(t))S(L(t))\right]N(L,t)dL \qquad \text{eqn 1}$$

where the closed interval Ω denotes the cell length domain. Note that this simple DEB-IPM does not account for temperature effects or reserve dynamics (which can, however, be an acceptable simplification [Jager et al. 2013]). Implicitly underlying the population-level model of eqn 1, like in any IPM, is a stochastic, individual-based model, in which individuals follow Markovian growth trajectories that depend on an individual's current state (Easterling et al. 2000). This individual variability is in standard IPMs modelled in the functions describing growth, $G(L',L(t))$, and the parent-offspring association, $D(L',L(t))$, using a probability density distribution, typically Gaussian (Easterling et al. 2000). In the DEB-IPM, this individual variability arises from how individuals experience the environment; specifically, the experienced feeding level Y follows a Gaussian distribution with mean $E(Y)$ and standard deviation $\sigma(Y)$. It means that individual cells within a cohort of length L do not necessarily experience the same feeding level due to demographic stochasticity (e.g. individuals, independently of each other, have good or bad luck in their feeding experience).

The survival function $S(L(t))$ in eqn 1 is the probability that an individual of cell length L survives from hour t to $t + 1$:

$$S(L(t)) = \begin{cases} (1 - p_D)e^{-\mu} & \text{for } L \leq L_m E(Y)/\kappa \\ 0 & \text{otherwise} \end{cases} \qquad \text{eqn 2}$$

assuming a constant background mortality rate μ (h^{-1}). The parameter L_m (μm) is the maximum cell length under conditions of unlimited abundance of food of the highest, relative quality, $E(Y) = 1$, and

κ is the fraction of ingested energy allocated to respiration. The probability of an individual dividing, and subsequently produce n_O = 2 offspring, p_D, enters the survival function to represent binary fission (Margolin, 2005), because reproduction in microorganisms entails that the dividing individual ceases to exist. Individuals die from starvation at a cell length at which maintenance requirements exceed the total amount of assimilated energy, which occurs when $L > L_m \cdot E(Y)/\kappa$ and hence, then, $S\big(L(t)\big) = 0$ (e.g., an individual of size L_m will die of starvation if $E(Y) < \kappa$).

The function $G(L', L(t))$ is the probability that an individual of cell length L (μm) at hour t grows to length L' at t + 1, conditional on survival, and follows a Gaussian distribution (Easterling et al. 2000):

$$G(L', L(t)) = \frac{1}{\sqrt{2\pi\sigma_L(L(t+1))}} e^{\frac{-(L'-E(L(t+1))^2}{2\sigma_L^2(L(t+1))}} \qquad \text{eqn 3}$$

with

$$E\big(L(t+1)\big) = L(t)e^{-\dot{r}_B} + \big(1 - e^{-\dot{r}_B}\big)L_m \cdot E(Y), \qquad \text{eqn 4}$$

and

$$\sigma^2(L(t+1)) = (1 - e^{-\dot{r}_B})^2 L_m^2 \sigma^2(Y), \qquad \text{eqn 5}$$

where $\dot{r}_B$ is the von Bertalanffy growth rate and $\sigma(Y)$ is the standard deviation of the expected feeding level, assuming individuals can shrink under starvation conditions.

The reproduction function $R(L(t))$ follows a 'pre-breeding' census as cell division, i.e. reproduction, is fatal. $R(L(t))$ gives the number of offspring produced between hour t and t + 1 by an individual of cell length L (μm) at hour t:

$$R(L(t)) = \begin{cases} 0 & \text{for } L_b \leq L < L_d \\ n_O \cdot p_D & \text{for } L_d \leq L \leq L_m E(Y)/\kappa \end{cases} \qquad \text{eqn 6}$$

An individual always divides to produce n_O = 2 offspring [one parent and one offspring cell]. We set the cell length at which individuals divide, L_d (μm), equal to the asymptote of the von Bertalanffy growth curve in cell length so that $L_d = E(Y) \cdot L_m$. Only surviving adults reproduce; thus, only individuals within a cohort of cell length $L_d \leq L \leq L_m Y/\kappa$ reproduce. The probability of an individual dividing, p_D, equals:

$$p_D = \begin{cases} 0 & \text{for } L < L_d \\ 1 & \text{for } L \geq L_d \end{cases} \qquad \text{eqn 7}$$

Note that the probability of dividing also enters the survival function as division is fatal.

The probability density function $D(L', L(t))$ gives the probability that the offspring of an individual of cell length L are of length L' at hour t + 1:

$$D(L', L(t)) = \begin{cases} 0 & \text{for } L < L_d \\ \frac{1}{\sqrt{2\pi\sigma^2_{L_b}(L(t))}} e^{\frac{-(L' - E_{L_b}(L(t)))^2}{2\sigma^2_{L_b}(L(t))}} & \text{otherwise} \end{cases} \qquad \text{eqn 8}$$

Where $E_{L_b}(L(t))$ is the expected cell length of offspring produced by a cohort of individuals with length $L(t)$, and $\sigma^2_{L_b}(L(t))$ the associated variance. For simplicity, we set $E_{L_b}(L(t)) = L_b$ (μm) constant, and assumed its associated variance, $\sigma^2_{L_b}(L(t))$, to be negligibly small. Within species, offspring are thus evenly sized.

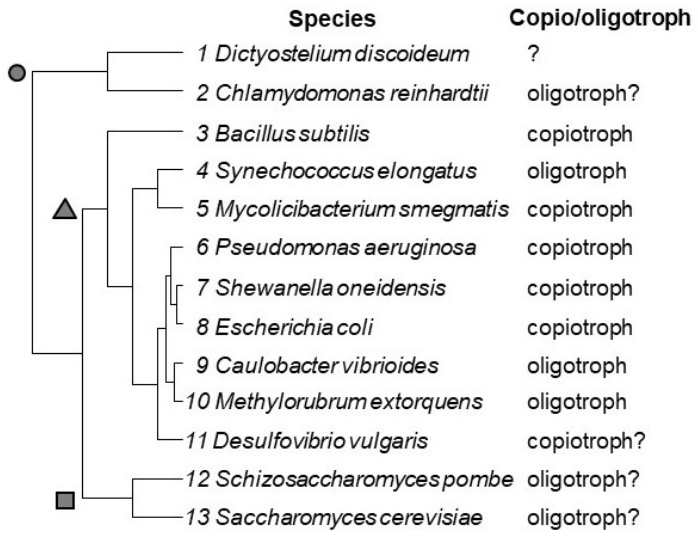

Figure 1. Phylogenetic tree of the 13 study species created using the *rotl* package (Michonneau et al., 2016) to download a tree from the Open Tree of Life (OTL) (Hinchliff et al., 2015), after taxonomical updating using the R library *taxize* (Chamberlain and Szocs, 2013) (input names of *Synechococcus elongatus, P. aeruginosa* and *Escherichia coli* were changed to *Synechoccocus elongatus* CCMP1630, *Pseudomonas aeruginosa* 148 and *Escherichia coli* 402290, respectively). Branch length was computed using the *compute.brlen* in the R package *ape* (Paradis et al., 2004). Polytomies were collapsed using the function *multi2di* in *ape* (Hinchliff et al., 2015). Copiotroph and oligotroph classification was according to Stone et al. 2023 for species 2-10, and suspected classifications (indicated with questions marks) are from Layboum-Perry et al. (1991) (species 2), Orellana et al. (2021) (species 11), and Ho et al. (2023) (species 12-13).

Parameterization of the DEB-IPM

The projection interval between time t and time $t + 1$ was set at 1 hour; all rates and durations are therefore expressed per hour, or in hours, respectively. We parameterized DEB-IPMs for 13 microorganisms (Fig. 1) (Table 1), setting κ, μ and n_0 at constant values: $\kappa = 0.9$ (for macro-organisms, κ is assumed to be 0.8; we assumed this would be higher for microorganisms as most energy goes into respiration and not reproduction and thus set it at 0.9), $\mu = 0.01\ h^{-1}$ (assuming background mortality under laboratory circumstances is very low), and $n_O = 2$ (as one microorganism

Table 1. Model parameters for the 13 microorganisms (see also Fig. 1). Parameters are expected feeding level $E(Y)$, the fraction of assimilated energy allocated to respiration, κ, cell length at birth, L_b, length at division, L_d, maximum length, L_m, mortality rate, μ, von Bertalanffy growth rate, $\dot{r}_B$, and number of offspring produced, n_O. Units are in brackets. Superscript numbers are references (see footnotes below). Species numbers are the same as in the Fig. 1. See further main text.

			Model parameters							
ID	**Species**	**Kingdom**	**E(Y)**	**κ**	L_b	L_d	L_m	**μ**	n_O	$\dot{r}_B$
			(–)	(–)	(μm)	(μm)	(μm)	(h^{-1})	(#)	(h^{-1})
1	*Dictyostelium discoideum*	Protista	0.80	0.90	15.26 [p]	24.74 [p]	48.48 [p]	0.01	2	0.12
2	*Chlamydomonas reinhardtii*	Plants	1.00	0.90	12.64 [q]	27.26 [q]	29.23 [q]	0.01	2	0.03
3	*Bacillus subtilis*	Bacteria	0.80	0.90	3.84 [l]	6.89 [l]	13.87 [l]	0.01	2	1.62
4	*Synechococcus elongatus*	Bacteria	1.00	0.90	2.04 [o]	5.98 [o]	8.031 [o]	0.01	2	0.03
5	*Mycobacterium smegmatis*	Bacteria	0.80	0.90	5.06 [e]	8.72 [e]	11.96 [f]	0.01	2	0.09
6	*Pseudomonas aeruginosa*	Bacteria	0.80	0.90	3.86 [i]	17.34 [i]	26.00 [j]	0.01	2	0.25
7	*Shewanella oneidensis*	Bacteria	0.80	0.90	1.35 [k]	3.35 [k]	5.00 [k]	0.01	2	0.17
8	*Escherichia coli*	Bacteria	0.50	0.90	2.18 [g]	3.46 [g]	8.00 [h]	0.01	2	5.21
9	*Caulobacter vibrioides*	Bacteria	0.70	0.90	1.76 [m]	3.22 [m]	5.30 [n]	0.01	2	1.10
10	*Methylorubrum extorquens*	Bacteria	0.90	0.90	1.71 [r]	4.40 [r]	5.24 [r]	0.01	2	0.15
11	*Desulfovibrio vulgaris*	Bacteria	1.00	0.90	3.15 [s]	6.18 [s]	6.19 [s]	0.01	2	0.49
12	*Schizosaccharomyces pombe*	Fungi	0.90	0.90	8.67 [a]	16.00 [a]	19.43 [b]	0.01	2	0.69
13	*Saccharomyces cerevisiae*	Fungi	0.99	0.90	3.78 [c]	8.12 [c]	8.24 [d]	0.01	2	0.56

[a] Buchwald and Sveiczer (2006); Sveiczer et al., (1997); [b] Nobs and Maerkl (2014); [c] Ferrezuelo et al., (2012); [d] Allard et al., (2018); [e] Priestman et al., (2017); [f] Aldridge et al., (2011); [g] Nieto et al., (2020); [h] Zheng et al., (2016); [i] Deforet et al., (2015); [j] Steel et al., (2004) [k] Lee et al., (2016); [l] Sauls et al., (2019); [m] Banerjee et al., (2017); [n] Beaufay et al., (2015); [o] Martins et al., (2018); [p] Tanaka and Yumura (2021); [q] Vitova et al., (2010); [r] Strovas et al., (2007); [s] Fiévet et al., (2015).

divides to produce two offspring) (Table 1). Values of L_b, L_d, L_m, and $\dot{r}_B$ were taken from the literature (references in Table 1) or estimated from other data. Specifically, in case of *S. cerevisiae*, we calculated cell length as the cell diameter $2r$ (μm) from cell volume V (μm^3), assuming *S. cerevisiae* cells are sphere-shaped so that $V = \frac{4}{3}\pi r^3$, from which follows that cell length equals $2r = 2\left(\frac{3}{4\pi}V\right)^{1/3}$. To calculate L_m for *S. cerevisiae*, we used the volume of a mother cell and bud (Allard et al., 2018), and subtracted the volume of the mother cell at division from the volume of the mother

191 cell at birth, assuming that the size at birth of the mother equals the bud's size. Cell length of the
192 mother and bud were calculated from the volume measures as before, and added together to give
193 maximum length, L_m, of *S. cerevisiae*. In case of *Chlamydomonas reinhardtii*, we assumed that, given
194 their shape, cells were proportioned as 4 × 4 × 10 µm (Rochaix 2013). Given the fact that cell volume
195 $V = \frac{4}{3}\pi r^3$ and $r^3 = 4a \cdot 4a \cdot 10a$, gives cell length as $10a = \sqrt[3]{3V/(640\pi)}$, where a is the ratio
196 between the 3 dimensions of the cell, making '10a' the longest cell dimension and therefore
197 interpretable as cell length. In case of *Mycobacterium smegmatis*, measures of cell length at birth
198 and the elongated length of a single cell were combined to give L_m. In case of *Pseudomonas*
199 *aeruginosa*, only log values of cell length were available (Deforet et al., 2015), which we
200 backtransformed. Cell length measures of *Bacillus subtilis* were available for different media, and we
201 used those values obtained for cells grown on a favourable, glycerol rich medium (Sauls et al., 2019).
202 In case of *Dictyostelium discoideum*, we inferred from photos that cells are circle-shaped in between
203 birth and mitosis (Tanaka and Yumura, 2021), so that cell surface $S = \pi r^2$, from which follows that
204 the cell length equals $2r = 2\sqrt{S/\pi}$. Cell surfaces measures to calculate cell lengths of *D. discoideum*
205 were taken from two time frame photos taken between mitosis and birth (Tanaka and Yumura,
206 2021). Finally, we manually measured cell lengths of *Desulfovibrio vulgaris* from a series of scale-
207 barred images of cell length over time (Fiévet et al., 2015). For all species, we estimated the von
208 Bertalanffy growth rate, $\dot{r}_B$, using a nonlinear least-squares estimation procedure in R (nls function)
209 (R Core Team 2021) to fit the equation $L_t = L_d - [L_d - L_b]e^{-\dot{r}_B t}$ for $\dot{r}_B$ (Smallegange et al., 2017)
210 against observed growth curves of cell length L_t (µm) over time t (hours), taken from the literature
211 (see R code in: Romeijn and Smallegange [2021]).
212

213 **Identifying life history patterns**

214 For each species, we used their DEB-IPM to calculate in MATLAB [version 9.10.01602886 R2021a]
215 seven representative life history traits: generation time T, the shape of the survivorship curve H, age
216 at maturity L_α, progressive growth γ, retrogressive growth ρ, mean recruitment success φ, and net

reproductive rate R_0 (Salguero-Gómez et al. 2016) (Table 2) that inform on schedules of survival, growth and reproduction. The equations to calculate these life history traits are in Table 2. Because all individuals die after reproducing, we did not include mature life expectancy or degree of iteroparity. We set $E(Y)$ for each species such that it mimics favourable laboratory conditions and

Table 2. Life history traits and their loadings onto the first two PC axes. To calculate life history traits, we discretised the IPM (Eqn 1) by dividing the length domain Ω into 200 very small-width discrete bins, resulting in a matrix **A** of size $m \times n$, where $m = n = 200$, and which dominant eigenvalue equals λ. Mean lifetime reproductive success R_0 is the dominant eigenvalue of the matrix $\mathbf{F} = \mathbf{V}(\mathbf{I} - \mathbf{GS})^{-1}$, where **I** is the identity matrix and **V** = **DR**, with **D** as the parent-offspring association, **R** the reproduction, **G** the growth and **S** the survival matrix (Caswell 2001); this gives generation time $T = \log(R_0)/\log(\lambda)$ (Caswell 2001). The mean life expectancy, η_e, is calculated as $\eta_e = \mathbf{1}^T\mathbf{N}$, where **1** is a vector of ones of length m and **N** is the fundamental matrix $\mathbf{N} = (\mathbf{I} - \mathbf{S})^{-1}$. The longevity of an individual of length L is η_L, which means we can calculate age at sexual maturity $L_\alpha = \eta_{L_b}$ and mature life expectancy $L_\varpi = \eta_{L_p}$ so that $\eta_e = L_\alpha + L_\varpi$ (Caswell 2018, eqn 4.21). l_x is the probability of surviving to age at least x, and m_x is the average fertility of age class x (cf. Tuljapurkar et al. 2009). $\bar{\mathbf{G}}$ is the mean of **G**, $\bar{\mathbf{V}}$ is the mean of **V,** and i and j are the row and column entries of the matrix, respectively. The vital rates included in the studied set of fundamental life history traits (progressive growth γ, retrogressive growth ρ, and sexual reproduction φ) were averaged across the columns j (the length bins), weighted by the relative contributions of each stage at stationary equilibrium. For example, to calculate mean sexual reproduction φ, we summed the values in the columns j of the **V** matrix and multiplied each φ_{ij} by the corresponding jth element w_j of the stable stage distribution **w**, calculated as the right eigenvector of **A**.

Life history trait	Symbol	Definition	Equation	p-PC1	p-PC2	p-PC3	PC1	PC2	PC3
Generation time	T	Number of hours required for the individuals of a population to be fully replaced by new ones	$T = \frac{\log(R_0)}{\log(\lambda)}$	**0.98**	-0.02	-0.08	0.48	-0.02	-0.07
Survivorship curve	H	Keyfitz' entropy ($H < 1$ denotes increasing mortality rate with age, $H > 1$ denotes decreasing mortality rate with age, $H = 1$ denotes a constant mortality rate with age) (Keyfitz & Caswell 2005).	$H = -\frac{\sum_{x=0}^{x=\eta_e} \log(l_x) l_x}{\sum_{x=0}^{x=\eta_e} l_x}$	0.45	**-0.78**	-0.33	0.22	**-0.70**	-0.31
Age at maturity	L_α	Number of hours that it takes an average individual in the population to become reproductive	$L_\alpha = \eta_{L_b}$	**0.98**	-0.06	-0.06	0.48	-0.05	-0.06

Progressive growth	γ	Mean probability of growing to a larger length across the length domain Ω.	$\gamma = \sum_{i}^{m} \bar{\mathbf{G}}_{i,j} \bar{\mathbf{w}}_j \vert_{i<j}$	**0.92**	0.24	0.05	0.44	0.21	0.04
Retrogressive growth	ρ	Mean probability of growing to a smaller length across the length domain Ω.	$\rho = \sum_{i}^{m} \bar{\mathbf{G}}_{i,j} \bar{\mathbf{w}}_j \vert_{i>j}$	**-0.53**	-0.25	**-0.78**	-0.26	-0.22	**-0.73**
Mean recruitment success	φ	Mean per-capita number of recruits across the length domain Ω.	$\varphi = \sum_{i}^{m} \bar{\mathbf{V}}_{i,j} \bar{\mathbf{w}}_j$	**-0.99**	0.04	0.07	-0.48	0.04	0.06
Net reproductive rate	R_0	Mean number of recruits produced during the mean life expectancy of an individual in the population.	$R_0 = \sum_{x=0}^{x=\eta_e} l_x m_x$	-0.16	**-0.72**	**0.65**	-0.08	**-0.65**	**0.60**

Loadings in bold indicate a high contribution (greater than ±0.50) of the life-history trait to the PC axis. p-PC axes are from the phylogenetically constructed PCA, and PC axes from a 'normal' PCA.

exponential growth, so that $\lambda > 1$ and $R_0 > 1$ (Table 3). We evaluated the variation in these traits along major axes using phylogenetically corrected principal component analysis (p-PCA) (Revell 2012) conducted in R (R core team 2022) to identify the major life history strategy axes. To this end we used the *phyl.pca* function in the R library *phytools* (Revell 2012; Salguero-Gómez et al. 2016; Paniw et al. 2018), after log-transforming and scaling values to $\mu = 0$ and SD = 1 to agree with PCA assumptions.

We estimated Pagel's λ to inform on the phylogenetic correlation between species traits expected under Brownian motion (Freckleton et al., 2002), which varies between 0 (phylogenetic independence) and 1 (species traits covary proportionally to their shared evolutionary history). We used Pagel's λ because it has been used successfully in previous cross-taxonomical PCAs on life history traits (Salguero-Gómez et al. 2016; Paniw et al. 2018; Capdevila et al. 2020), it can describe the evolution of trait distributions in bacteria well (Haywood-Farmer & Otto 2003), and has been shown to suffer from a lower rate of type I error (and a low rate of type II error) for phylogenies of

235 varying sizes (Münkemüller et al. 2012). Pagel's λ is estimated jointly for all life history traits (Revell

236 2012). Note that Pagel's λ does not detect non-Brownian models of evolution. Non-Brownian

237 models of trait evolution exist that can yield phylogenetic dependence (λ = 1), like niche-filling

238 models that assume that traits change only at speciation in response to selection to exploit new

Table 3. The life history traits generation time *T*, survivorship curve *H*, age at sexual maturity L_α, progressive growth γ, retrogressive growth ρ, mean sexual reproduction φ, and net reproductive rate R_0 calculated from DEB-IPMs and analysed using PCAs (Table 2). Species numbers are the same as in Fig. 1.

	Species	**Life history trait**						
		T	H	L_α	γ	ρ	φ	R_0
1	*Dictyostelium discoideum*	6.11	0.11	5.69	4.29E-05	3.11E-08	0.24	1.69
2	*Chlamydomonas reinhardtii*	73.80	0.27	51.90	1.31E-04	2.35E-06	0.02	0.96
3	*Bacillus subtilis*	2.01	0.02	2.00	3.21E-05	3.49E-06	0.82	1.16
4	*Synechococcus elongatus*	37.54	0.15	31.00	1.73E-04	2.65E-09	0.04	1.32
5	*Mycobacterium smegmatis*	20.65	0.22	18.35	4.72E-05	2.75E-06	0.07	1.49
6	*Pseudomonas aeruginosa*	7.90	0.17	7.63	3.83E-05	8.32E-07	0.18	1.71
7	*Shewanella oneidensis*	10.04	0.18	9.50	3.72E-05	9.17E-07	0.14	1.71
8	*Escherichia coli*	2.27	0.16	2.32	2.13E-05	1.93E-05	0.71	1.20
9	*Caulobacter vibrioides*	2.88	0.21	2.89	2.86E-05	6.99E-06	0.54	1.39
10	*Methylorubrum extorquens*	16.45	0.23	15.20	4.48E-05	2.07E-06	0.09	1.57
11	*Desulfovibrio vulgaris*	8.59	0.34	8.55	5.78E-05	5.40E-06	0.17	1.52
12	*Schizosaccharomyces pombe*	4.24	0.22	4.20	3.87E-05	3.86E-06	0.35	1.50
13	*Saccharomyces cerevisiae*	7.79	0.33	7.81	5.74E-05	5.34E-06	0.18	1.51

239

240 niches (Price 1997; Harvey & Rambaut 2000). Intermediate levels of phylogenetic dependence (0 < λ

241 < 1) could result from the mode of evolution represented by models such as the Ornstein-Uhlenbeck

242 model (e.g, Hansen 1997; Martins & Hansen 1997), in which the influence of phylogeny decays

243 through time because species trait values tend to be pulled back toward an evolutionary optimum

244 irrespective of the starting point, or even result from measurement error (Freckleton et al. 2012). In

245 the simplest, non-Brownian model, traits may evolve instantaneously in response to selection, in

246 which case traits would show no phylogenetic dependence (λ = 0). Additional tests are required to

distinguish these forms of models. Because it turned out that Pagel's λ was close to 0, we also carried a normal PCA on the life history traits. We assessed the significance of PC axes using Kaiser's criterion [Legendre and Legendre, 2012]).

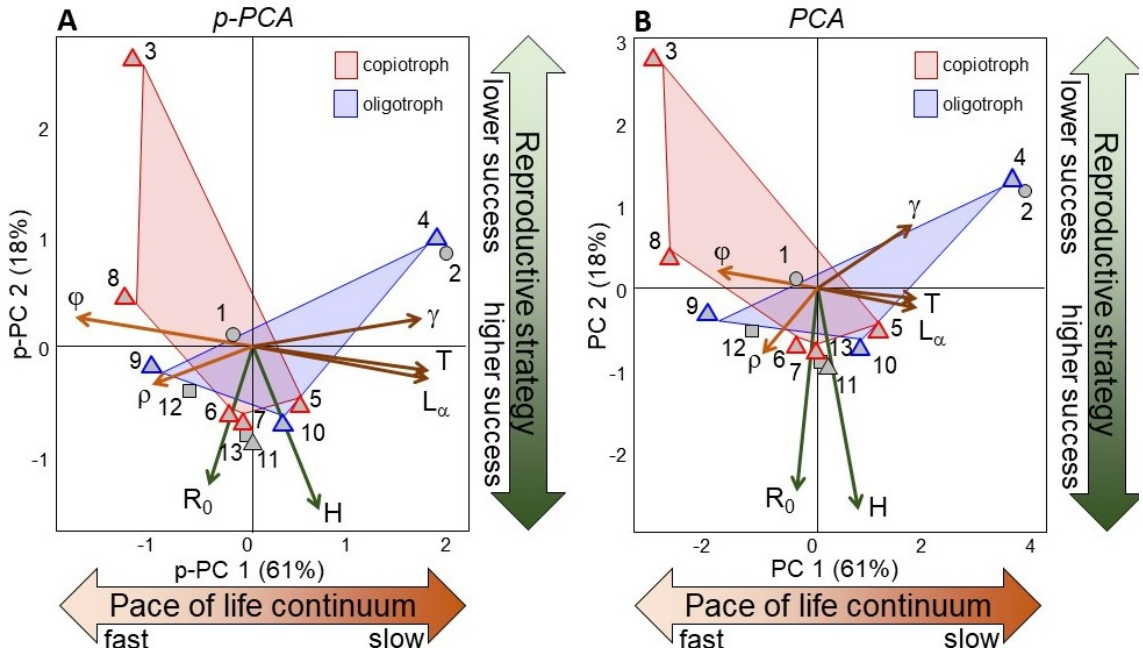

Figure 2. To characterise life histories, a phylogenetically informed PCA (p-PCA) (**A**) and a normal PCA (**B**) was performed on generation time *T*, the shape of the survivorship curve *H*, age at maturity L_α, progressive growth γ, retrogressive growth ρ, mean recruitment success φ, and net reproductive rate R_0 (Table 3). Both show the same result. In both cases, we show the first two PC axes, although the eigenvalue of the third PC axis was also > 1 (following the Kaiser criterion [Legendre and Legendre, 2012]: $\lambda_{axis\ 1} = 4.27$; $\lambda_{axis\ 2} = 1.25$; $\lambda_{axis\ 3} = 1.15$; $\lambda_{axis\ 4} = 0.25$) and the third axis explained 16% of the variation (see further main text). Arrow lengths are proportional to the loadings of each trait onto these two axes. Circles indicate protist or plant, triangles indicate bacteria, and squares indicate fungi. Numbers next to symbols indicate species identity as in Fig. 1 and in Tables 1 and 3. Confirmed classifications of species as copiotroph (red-lined symbols) and oligotroph (blue-lined symbols) (Fig. 1) are indicated in both biplots and the associated convex hulls denote areas of life history strategy space occupied by them.

Results

The range of microorganismal life history traits was captured by the first three p-PC axes of the p-PCA, which together explained 79% of the variation (Fig. 2A). The life history traits most closely aligned with p-PC1 are related to the fast-slow continuum (Stearns 1992): generation time (T), age at maturity (L_α) and mean recruitment success (φ) had the greatest loadings onto p-PC1. The positive loading of generation time onto p-PC1 had an opposite loading for mean recruitment success, supporting a tradeoff between highly reproductive species and population turnover (Stearns 1992) (Table 2). The rate of individual cell growth (progressive growth, γ) and shrinkage (retrogressive growth, ρ) also loaded onto p-PC1 (Table 2). Thus, as we move from negative to positive scores along p-PC1, individuals increase their allocation to individual growth and to the longevity-related life history trait age at maturity and decrease in population turnover (i.e., greater generation time) at the expense of the production of new recruits (Fig. 2A). Only at the extreme ends of this pace of life continuum was there a match between copiotrophs at the fast end and oligotrophs at the slow end of the continuum (red (copiotroph) and blue (oligotroph) convex hulls do not overlap at the extreme ends in Fig. 2A).

The two life history traits aligned with p-PC2 represent dimensions of microorganism reproductive strategy not captured by mean recruitment success: both the net reproductive rate (R_0) and the shape of the survivorship curve (H) are negatively loaded onto p-PC2: the reproductive strategy axis (Table 2). This means that, as we move from positive to negative scores along p-PC2, microorganisms attain greater lifetime reproductive success while the mortality of older individuals decreases. This time, there was almost complete overlap between species classified as copiotrophs and oligotrophs along the reproductive strategy axis (red and blue convex hulls in Fig 2A, respectively).

Interestingly, p-PC3 is retained [its associated eigenvalue >1 (Fig. 2A)] and explained 16% of the variation. The negative loading of net reproductive rate R_0 onto p-PC3 had an opposite loading

for retrogressive growth ρ (Table 2): moving from one end of p-PC3 to the other, microorganisms attain greater (or lower) lifetime reproductive success and tend to shrink less (or more).

Finally, there was a weak phylogenetic signature in the structuring of life history variation (Pagel's λ was close to zero: $\lambda < 0.01$), suggesting a weak role of overall phylogenetic ancestry in life history trait variation, confirmed by traitgrams that showed no strong mapping of a species' place along the pace of life continuum (Fig. 3A) or reproductive strategy axis (Fig. 3B) and its phylogenetic position. We therefore ran a normal PCA, which showed the same results as the p-PCA (Table 3, Fig. 2B).

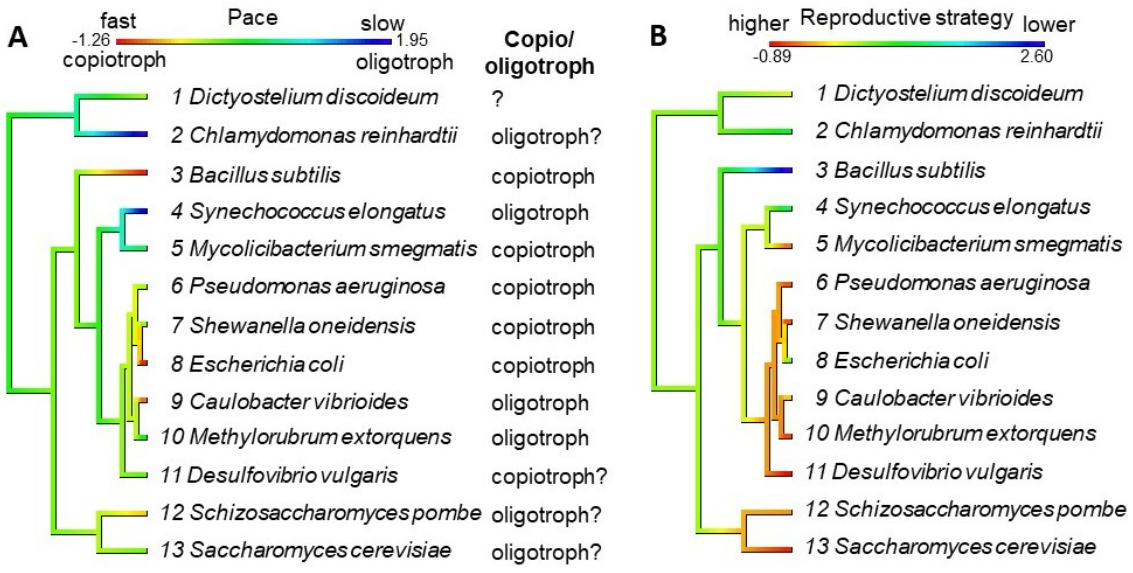

Figure 3. Traitgrams indicating the relationship between a species' phylogenetic position (as in Fig. 1) and (**A**) its place along the pace of life continuum from fast (negative values in red) to slow (positive values in blue), and (**B**) its place along the reproductive strategy axis from high success (negative values in red) to low success (positive values in blue). Values in (A) are the scores of p-PC1 and values in (B) are the scores of p-PC2 (Fig. 2A). Copiotroph and oligotroph classification was according to Layboum-Perry et al. (1991) (species 1), Stone et al. 2023 (species 2-10), Orellana et al. (2021) (species 11), and Ho et al. (2023) (species 12-13) (questions marks indicate suspected classifications).

305 **Discussion**

306 Microorganisms are typically classified as copiotroph or oligotroph but it has been proven difficult to
307 generalise their life history strategies to broad lineages (Stone et al. 2023). Here, we assessed if the
308 fast-slow reproductive strategy framework, which has so far only applied to animals and higher
309 plants (Salguero-Gómez et al., 2016; Paniw et al., 2018; Capdevila et al., 2020; Smallegange et al.,
310 2020), can be applied to microorganisms. We also tested if inferences about life history strategies
311 can be made from patterns in taxonomic composition of microorganisms. Like animals and higher
312 plants, we found that microorganismal life history variation was structured along a fast-slow pace of
313 life continuum and an axis of reproductive strategy (Gaillard et al., 1989; Salguero-Gómez et al.,
314 2016). But only at the extreme ends of the pace of life continuum was there a match between
315 copiotrophs at the fast end and oligotrophs at the slow end of the continuum. Our explorative work
316 therefore suggests that the fast-slow reproductive strategy framework can provide a strong
317 predictive framework on the behaviour and activity of microorganism than can to some extent be
318 used alongside the copiotroph-oligotroph dichotomy.

319 Like previous life history strategy analyses on animals and higher plants, we found that our
320 findings of microorganismal life history strategies were unaffected by phylogeny. It could be that
321 plasticity in life history traits (variation of trait values within a species that occurs in response to
322 variability in the environment) is obscuring the phylogenetic signal. For example, microorganisms
323 can switch from fermentation to respiration in response to changes in glucose availability, resulting
324 in great reprogramming of gene expression (e.g., Roberts and Hudson 2006). Also, cell growth in e.g.,
325 *S. cerevisiae* and *B. subtilis* depends on food quality (Ferrezuelo et al., 2012; Sauls et al., 2019),
326 creating plasticity in growth. When variation among individuals in a species is sufficiently large to
327 approach variation between species, any correlation between species traits and their evolutionary
328 relatedness can be masked. Alternatively, or additionally, the lack of a phylogenetic signal may be
329 due to high life history trait lability (e.g., Savage and Cavender-Bares 2012), or due to weak links
330 between genotype and phenotype evolution mapping as life history traits are typically determined

331 by multiple genes that interact to produce phenotypes in a non-additive or non-linear fashion (e.g,
332 Zörgö et al. 2012). If indeed phylogenetic relationships play a minimal role in determining life history
333 adaptations of microorganisms, environmental filtering stemming from extrinsic factors should be
334 considered as the main process of the evolution of microorganismal life history strategies (Stearns
335 1992).

336 The evolution of life history strategies is also shaped by the tradeoffs that individual make
337 between investment into survival, growth and reproduction (Stearns, 1992). Firstly, the pace of life
338 continuum in animals and higher plants is underpinned by a tradeoff between fast-growing, highly
339 reproductive species and population turnover (Salguero-Gómez et al., 2016; Paniw et al., 2018). We
340 also found that the microorganismal pace of life continuum was underpinned by a tradeoff between
341 highly reproductive species and population turnover, but the highly reproductive species were
342 associated with low values of progressive growth (γ), and, thus, fast microorganisms were slower,
343 and not faster growers. This result can perhaps be explained by the fact that individual growth in
344 microorganisms is an increase in cell size but in macroorganisms, among others, an increase in total
345 cell mass (Conlon and Raff, 1999). Secondly, a tradeoff between current and future reproduction
346 underlies the reproductive strategy axis (Charnov and Schaffer, 1973; Shaw and Levin, 2013). Highly
347 semelparous species with a single reproductive event in their lifespan and high mortality are ranked
348 at one extreme, and iteroparous species with high spread in reproduction and low mortality on the
349 other (Healy et al., 2019). We did find, like animals and higher plants, that the reproductive strategy
350 axis captured variation in net reproductive rate (R_0), but we modelled a semelparous life history
351 strategy for all the microorganisms in our study (as an individual cell divides (and 'dies') to produce
352 an offspring and parent cell) (Campos et al*.,* 2014; Taheri-Araghi et al*.,* 2015; Sauls et al*.,* 2016).
353 However, the plant *C. reinhardtii*, the fungi *S. pombe* and *S. cerevisiae*, and the protist *D. discoideum*
354 can reproduce sexually (Nielsen 2004; Urushihara and Muramoto, 2006; Wallen and Perlin, 2018).
355 Also, when reproducing asexually, *S. cerevisiae* divides via budding, producing a smaller offspring cell
356 and a remaining, larger parent cell. The plant *C. reinhardtii*, in turn, undergoes a multiple-fission

357 cycle, potentially producing up to eight daughter cells (Cross and Umen, 2015). Future endeavours
358 could explore how more complex growth and reproduction patterns affect life history strategy
359 structuring.

360 In conclusion, we identified a pace of life and reproductive strategy axis in microorganisms,
361 albeit for a small number of species. Next steps should at least (i) target more species, including
362 from the field, (ii) systematically control abiotic factors like temperature, and (iii) explore a variety of
363 growth and reproduction patterns. We hope that our first exploration will ignite such research. It
364 could help us understand the diversity of microorganismal phenotypes (Keymer et al., 2006;
365 Santillan et al., 2019; Kiørboe & Thomas, 2020), and increase our understanding of how they impact
366 on higher level processes like host phenotype expression (Kopecky et al., 2014; Zindel et al., 2017),
367 and human physiology and metabolism (de Vrieze et al., 2013; Rook et al., 2017).

368

369 **Author contributions**

370 **Josje Romeijn**: data collection, formal analysis, visualisation, and writing of the first draft. **Isabel M.**
371 **Smallegange**: conceptualisation, supervision and writing of final draft.

372

373 **Data availability statement**

374 Supplemental data, R code and MatLab code is available as an Online Appendix at
375 https://doi.org/10.6084/m9.figshare.16831543.v2 (Romeijn and Smallegange [2021]).

376

377 **Conflict of interest**

378 The authors declare they have no conflict of interest relating to the content of this article. IMS is a
379 recommender for PCI Zoology.

380

381 **Funding**

382 This work received no funding.

References

Aldridge, B. et al. 2011. Asymmetry and aging of mycobacterial cells lead to variable growth and antibiotic susceptibility. - Science 335: 100–104.

Allard, C. et al. 2018. A size-invariant bud-duration timer enables robustness in yeast cell size control. – PloS One 13: e0209301

Banerjee, S. et al. 2017. Biphasic growth dynamics control cell division in *Caulobacter crescentus*. - Nature Microbiology 2: 17116.

Beaufay, F et al. (2015). A NAD-dependent glutamate dehydrogenase coordinates metabolism with cell division in *Caulobacter crescentus*. - The EMBO journal, 34: 1786-1800.

Buchwald, P. and Sveiczer, A. (2006). The time-profile of cell growth in fission yeast: Model selection criteria favoring bilinear models over exponential ones. - Theor. Biol. Med. Mod. 3:16.

Campos, M. et al. 2014. A constant size extension drives bacterial cell size homeostasis. – Cell 159:1433-1446.

Capdevilla, P. Beger, M., Blomberg, S.P., Hereu, B., Linares, C., and Salguero-Gómez, R. 2020. Longevity, body dimension and reproductive mode drive differences in aquatic versus terrestrial life history strategies. – Funct. Ecol. 34: 1613–1625.

Caswell, H. 2001. Matrix Population Models. Sunderland, MA: Sinauer Associates.

Caswell, H. 2018. Sensitivity analysis: Matrix Methods in Demography and Ecology. Demographic Research Methods. Springer Open.

Chamberlain, S. andSzocs, E. 2013. taxize - taxonomic search and retrieval in R. - F1000Research 2: 191.

Charnov, E.L., and Schaffer, W.M. 1973. Life-history consequences of natural selection: Cole's result revisited. - Am. Nat. 107:791–793

Conlon, I., and Raff, M. 1999. Size control in animal development. Cell 96: 235-244.

Cross, F. and Umen, J. 2015. The chlamydomonas cell cycle. - Plant J. 82: 370-392.

Deforet, M. et al. 2015. Cell-size homeostasis and the incremental rule in a bacterial pathogen. - Biophys. J. 109: 521–528.

Easterling, M.R., Ellner, S.P., and Dixon, P.M. 2000. Size-specific sensitivity: applying a new structured population model. - Ecology 81:694–708

Evans, S. and Wallenstein, M. 2013. Climate change alters ecological strategies of soil bacteria. - Ecol. Lett. 17: 155-164.

Ferrezuelo, F. et al. 2012. The critical size is set at a single-cell level by growth rate to attain homeostasis and adaptation. - Nature Comm. 3: 1012.

Fierer, N., Bradford, M.A., and Jackson, R.B. 2007. Toward an ecological classification of soil bacteria. Ecology 88:1354–1364.

Fiévet, A. 2015. Single-cell analysis of growth and cell division of the anaerobe *Desulfovibrio vulgaris* Hildenborough. - Front Microbiol. 6: 1378.

Freckleton, R.P. et al. 2002. Phylogenetic analysis and comparative data: a test and review of evidence. – Am. Nat. 160: 712–726.

Gaillard, J.-M. et al. 1989. An analysis of demographic tactics in birds and mammals. - Oikos 56: 59–76.

Hansen, T. F. 1997. Stabilizing selection and the comparative analysis of adaptation. Evolution 51:1341–1351.

Harvey, P.H. and Rambaut, A. 1998. Phylogenetic extinction rates and comparative methodology. Proceedings of the Royal Society of London B, Biological Sciences 265:1691–1696.

Haywood-Farmer, E., and Otto, S.P. 2003. The evolution of genomic base composition in bacteria. Evolution 57: 1783-1792.

Healy, K. et al. 2019. Animal life history is shaped by the pace of life and the distribution of age-specific mortality and reproduction. - Nature Ecol. Evol. 3: 1217-1224.

Hinchliff, C.E. et al. 2015. Synthesis of phylogeny and taxonomy into a comprehensive tree of life. – Proc. Natl. Acad. Sci. USA 112: 201423041.

Ho, A.,Di Lonardo, D.P., Bodelier, P.L.E. 2023. Revisiting life strategy concepts in environmental microbial ecology, FEMS Microbiology Ecology 93: fix006.

Jager, T. et al. 2013. DEBkiss or the quest for the simplest generic model of animal life history. - J. Theor. Biol. 328:9-18.

Kiørboe, T. and Thomas, M.K. 2020. Heterotrophic eukaryotes show a slow-fast continuum, not a gleaner–exploiter trade-off. - Proc. Natl. Acad. Sci. USA 117: 24893-24899.

Keyfitz, N. and Caswell, H. 2005. Applied mathematical demography. Springer, third edition edn.

Keymer, J.E. 2006. Bacterial metapopulations in nanofabricated landscapes. – Proc. Natl. Acad. Sci. USA 103: 17290-17295.

Koch, A.L. 2001. Oligotrophs versus copiotrophs. - BioEssays 23:657–61.

Kooijman, S.A.L.M., and Metz, J.A.J. 1984. On the dynamics of chemically stressed populations: the deduction of population consequences from effects on individuals. - Ecotoxicol. Environ. Saf. 8, 254–274.

Kopecky, J. et al. 2014. The effect of antibiotics on associated bacterial community of stored product mites. - PLoS ONE 9: e112919

Layboum-Parry, J., Marchant, H.J. Brown, P. 1991. The plankton of a large oligotrophic freshwater Antarctic lake. Journal of Plankton Research 13: 1137–1149.

Lee, C.K. et al. 2016. Evolution of Cell Size Homeostasis and Growth Rate Diversity during Initial Surface Colonization of *Shewanella oneidensis*. - ACS Nano 10:9183-9192.

Legendre, P. and Legendre, L. 2012. Numerical Ecology, 3rd ed. Elsevier, London, pp. 1006.

Margolin, W. 2005. Ftsz and the division of prokaryotic cells and organelles. – Nat. Rev. Mol. Cell Biol. 6: 862–71.

Martins, B.M.C. et al. 2018. Cell size control driven by the circadian clock and environment in cyanobacteria. - Proc. Natl. Acad. Sci. USA 115: E11415-E1142.

Martins, E.P. and Hansen, T.F. 1997. Phylogenies and the comparative method: a general approach to incorporating phylogenetic information into the analysis of interspecific data. – Am. Nat. 149:646–667.

Meistertzheim, A.-L. et al. 2016. Patterns of bacteria-host associations suggest different ecological strategies between two reef building cold-water coral species. - Deep Sea Res Part I 114: 12–22.

Michonneau, F. et al. 2016. rotl, an R package to interact with the Open Tree of Life data. - PeerJ Preprints 4:e1471v3.

Münkemüller T., Lavergne S., Bzeznik B., Dray S., Jombart T., Schiffers K., and Thuiller W. 2012. How to measure and test phylogenetic signal. Methods in Ecology and Evolution 3: 743– 756.

Nielsen, O. 2004. Mating-Type Control and Differentiation. In: Egel R. (eds) The Molecular Biology of *Schizosaccharomyces pombe*. Springer, Berlin, Heidelberg.

Nieto, C. et al. 2020. Unification of cell division control strategies through continuous rate models. – Phys. Rev. E 101: 022401.

Nobs, J.-B. and Maerkl, S. 2014. Long-term single cell analysis of *S. pombe* on a microfluidic microchemostat array. – PloS ONE 9: e93466.

Orellana, R., Arancibia, A. Badilla, L., Acosta, J., Arancibia, G., Escar, R., Ferrada, G., Seeger, M. 2021. Ecophysiological features shape the distribution of prophages and CRISPR in sulfate reducing prokaryotes. Microorganisms 9: 931.

Paniw, M., Ozgul A., and Salguero-Gómez R. 2018. Interactive life-history traits predict sensitivity of plants and animals to temporal autocorrelation. – Ecol. Lett. 21: 275–286.

Paradis, E. et al. 2004. APE: Analyses of phylogenetics and evolution in R language. – Bioinformatics 20: 289–290.

Price, T. 1997. Correlated evolution and independent contrasts. Philosophical Transactions of the Royal Society of London B, Biological Sciences 352:519–529.

Priestman, M. et al. 2017. Mycobacteria modify their cell size control under sub-optimal carbon sources. – Front. Cell Dev. Biol. 5:64.

R Core Team (2021) R: A language and environment for statistical computing. R Foundation for Statistical Computing, Vienna, Austria.

Ramin, K.I. and Allison, S.D. 2019. Bacterial tradeoffs in growth rate and extracellular enzymes. – Front. Microbiol. 10: 2956.

Revell, L.J. 2012. phytools: An R package for phylogenetic comparative biology (and other things). - Methods Ecol. Evol. 3: 217–223.

Roberts, G.G. and Hudson, A.P. 2006. Transcriptome profiling of Saccharomyces cerevisiae during a transition from fermentative to glycerol-based respiratory growth reveals extensive metabolic and structural remodeling. Mol. Genet. Genomics 276: 170–186

Rochaix, J.-D. 2013. *Chlamydomonas reinhardtii*. In S. Maloy and K. Hughes, editors, Brenner's Encyclopedia of Genetics (Second Edition), pages 521–524. Academic Press, San Diego, second edition.

Romeijn, J., and Smallegange, I.M., 2021: Exploring how the fast-slow pace of life continuum and cell size structure microorganism life history variation. figshare. Online resource. https://doi.org/10.6084/m9.figshare.16831543.v2

Rook, G. et al. 2017. Evolution, human-microbe interactions, and life history plasticity. - Lancet 390: 521–30.

Salguero-Gómez, R., Jones, O. R., Jongejans, E., Blomberg, S. P., Hodgson, D. J., Mbeau-Ache, C., … Buckley, Y. M. 2016. Fast–slow continuum and reproductive strategies structure plant life-history variation worldwide. - Proc. Natl. Acad. Sci. USA 113: 230–235.

Santillan, E. et al. 2019. Trait-based life-history strategies explain succession scenario for complex bacterial communities under varying disturbance. - Environ. Microbiol 21: 3751-3764.

Sauls, J.T. et al. 2016. Adder and a coarse-grained approach to cell size homeostasis in bacteria. – Curr. Opin. Cell Biol. 38: 38–44.

Sauls, J.T. et al. 2019. Control of *Bacillus subtilis* replication initiation during physiological transitions and perturbations. – mBio 10:e02205-19.

Savage, J.A., and Cavender-Bares, J. 2012. Habitat specialization and the role of trait lability in structuring diverse willow (genus *Salix*) communities. - Ecology 93: S138–S150.

Shaw, A.K., and Levin, S.A. 2013. The evolution of intermittent breeding. - J. Math. Biol. 66:685–703.

Smallegange, I.M. et al. 2017. Mechanistic description of population dynamics using dynamic energy budget theory incorporated into integral projection models. - Methods Ecol. Evol. 8: 146-154.

Smallegange, I.M. et al. 2020. Unusually paced life history strategies of marine megafauna drive atypical sensitivities to environmental variability. - Frontiers Mar. Sci. 7:597492.

Stearns, S.C. 1992. The Evolution of Life Histories. Oxford University Press, New York.

Steel, C. et al. 2004. Single live cell imaging of chromosomes in chloramphenicol-induced filamentous *Pseudomonas aeruginosa*. - Biochemistry 43: 175–182.

Stone, B.W.G., Dijkstra, P., Finley, B.K. et al. 2013. Life history strategies among soil bacteria—dichotomy for few, continuum for many. - ISME J.

Strovas, T. et al. 2007. Cell-to-cell heterogeneity in growth rate and gene expression in *Methylobacterium extorquens* AM1. – J. Bacteriology 189: 7127–7133.

Sveiczer, A. et al. 1997. The size control of fission yeast revisited. J. Cell Sci. 109: 2947–2957.

Taheri-Araghi, S. et al. 2015. Cell-size control and homeostasis in bacteria. – Curr. Biol. 25:385-391.

Tanaka, M. and Yumura, S. 2021. A 'dynamic adder model' for cell size homeostasis in *Dictyostelium* cells. – Sci. Rep. 11: 13742.

Tuljapurkar, S., Gaillard, J.M., and Coulson, T. 2009. From stochastic environments to life histories and back. – Phil. Trans. Roy. Soc. B. 364: 1499-1509.

Urushihara, H. and Muramoto, T. 2006. Genes involved in *Dictyostelium discoideum* sexual reproduction. – Europ. J. Cell Biol. 85: 961–968.

Vitova, M. et al. 2010. *Chlamydomonas reinhardtii*: Duration of its cell cycle and phases at growth rates affected by light intensity. - Planta 233: 75–86.

Vrieze, de Groot, P.F. et al. 2013. Fecal transplant: A safe and sustainable clinical therapy for restoring intestinal microbial balance in human disease? - Best Pract. Res. Clin. Gastroenterol. 27: 127-137.

Wallen, R. and Perlin, M. 2018. An overview of the function and maintenance of sexual reproduction in dikaryotic fungi. - Frontiers Microbiol. 9: 503.

Zheng, H. et al. 2016. Interrogating the *Escherichia coli* cell cycle by cell dimension perturbations. - Proc. Natl. Acad. Sci. USA 113: 15000-15005.

Zindel, R. et al. 2017. The role of the bacterial community in the nutritional ecology of the bulb mite *Rhizoglyphus robini* (Acari: Astignmata: Acaridae). - FASEB J. 27: 1488-1497.

Zörgö, E., Gjuvsland, A., Cubillos, F.A., Louis, E.J., Liti, G., Blomberg, A., Omholt, S.W., and Warringer, J. 2012. Life history shapes trait heredity by accumulation of loss-of-function alleles in Yeast. Mol. Biol. Evol. 29: 1781-1789.